

## Metabolic mapping of the primary visual system of the monkey by means of the autoradiographic [ $^{14}\text{C}$ ]deoxyglucose technique

(ocular dominance columns/blind spot/cerebral glucose utilization/cerebral energy metabolism/brain)

C. KENNEDY\*, M. H. DES ROSIERS†, O. SAKURADA†, M. SHINOHARA†, M. REIVICH‡, J. W. JEHLE†, AND L. SOKOLOFF†§

\* Department of Pediatrics, Georgetown University School of Medicine, Washington, D.C. 20007; † Laboratory of Cerebral Metabolism, National Institute of Mental Health, National Institutes of Health, Bethesda, Maryland 20014; and ‡ Department of Neurology, University of Pennsylvania School of Medicine, Philadelphia, Pa. 19174

Communicated by Seymour S. Kety, September 9, 1976

**ABSTRACT** An autoradiographic technique that employs 2- $^{14}\text{C}$ deoxyglucose to measure the local rates of glucose utilization within the brain has been applied to the binocular visual system of the Macaque monkey. This method, which pictorially displays the relative rates of glucose consumption in the component structures of the brain, delineates the regions of altered functional activity because of the close relationship between functional activity and energy metabolism. Bilateral retinal stimulation results in the delineation of different rates of glucose consumption in at least four cytoarchitectural layers of the striate cortex. The most intense metabolic activity appears to be in Layer IV, the locus of the termination of the geniculocortical pathway. Bilateral visual occlusion lowers the rates of glucose consumption in the striate cortex and markedly reduces the metabolic differentiation of the various layers. Unilateral visual deprivation delineates the laminae of the lateral geniculate body and the ocular dominance columns of the striate cortex. It also results in the autoradiographic visualization of regions with normally monocular input in the striate cortex, such as the rostral portions of the mushroom-like configurations in the calcarine cortex, which represent the extreme temporal crescents of the visual fields, and small regions in the most caudal part of the mushroom configurations, which are believed to represent the cortical loci of the blind spots of the visual fields.

Previous studies of the binocular visual system in the Macaque monkey have demonstrated the persistence of monocular representation of retinal units of the two eyes throughout the visual pathways from the lateral geniculate ganglia to the striate cortex (1-4). Although each retina projects more or less equally to both hemispheres, their projections remain segregated and terminate in six well-defined laminae in the lateral geniculates, three each for the ipsilateral and contralateral eyes (2-4). This segregation is preserved in the optic radiations which project the monocular representations of the two eyes for any segment of the visual field to adjacent regions of Layer IV of the striate cortex (1, 2). The cells responding to the input of each monocular terminal zone are distributed transversely through the thickness of the striate cortex resulting in a mosaic of columns, 0.3-0.5 mm in width, alternately representing the monocular inputs of the two eyes. The nature and distribution of these ocular dominance columns have previously been characterized by electrophysiological techniques (1), Nauta degeneration methods (2), and by autoradiographic visualization of axonal and transneuronal transport of [ $^3\text{H}$ ]proline- and [ $^3\text{H}$ ]fucose-labeled protein and/or glycoprotein (3, 4).

We recently described a method for the simultaneous measurement of the rates of glucose consumption in most of the macroscopic structural components of the brain (5-7). The method is based on the accumulation of 2-deoxy-D- $^{14}\text{C}$ glu-

cose-6-phosphate in the tissues after an intravenous pulse of 2-deoxy-D- $^{14}\text{C}$ glucose. Deoxyglucose is transported across the blood-brain barrier by the same carrier that transports glucose, and it competes with glucose for hexokinase, the enzyme that phosphorylates both. The rate of [ $^{14}\text{C}$ ]deoxyglucose phosphorylation is, therefore, quantitatively related to the rate of glucose phosphorylation and depends on the relative concentrations of both in the precursor pools and the kinetic constants of hexokinase for the two substrates. In a steady state of glucose metabolism, the net rate of glucose phosphorylation equals the rate of glucose utilization. Glucose consumption can then be calculated by means of an equation that defines it in terms of the time course of the relative concentrations of [ $^{14}\text{C}$ ]deoxyglucose and glucose in the plasma, the final tissue concentration of [ $^{14}\text{C}$ ]deoxyglucose-6-phosphate, the fractional turnover rate of the free [ $^{14}\text{C}$ ]deoxyglucose pool in the tissue, and the ratios of the Michaelis-Menten kinetic constants of hexokinase for deoxyglucose and glucose (6). The key to the localization possible with the method is a quantitative autoradiographic technique for the measurement of local tissue concentrations of [ $^{14}\text{C}$ ]deoxyglucose-6-phosphate. Even without the quantification, however, the autoradiographs are themselves pictorial representations of the local rates of glucose consumption throughout the brain. Inasmuch as local energy metabolism in the brain, as in other tissues, is closely coupled to local functional activity, the method has proved effective for the delineation of local cerebral regions with altered functional activity in response to experimentally modified physiological states (7).

The binocular visual system of the monkey appeared to offer an appropriately intricate and complex pattern of functional organization to test the capacity of the [ $^{14}\text{C}$ ]deoxyglucose method to define cerebral regions of altered functional activity. We have, therefore, applied the [ $^{14}\text{C}$ ]deoxyglucose technique to map and demonstrate pictorially on the basis of local metabolic rate the distribution of monocular representation in the monkey brain.

### METHODS

Rhesus monkeys of either sex weighing 2.5-3.5 kg were used in these studies. Polyethylene catheters were inserted in a femoral artery and vein after light halothane and nitrous oxide anesthesia, and the animals were then placed in a restraining chair and allowed to recover from the anesthesia for at least 4 hr. The experimental period was initiated by the intravenous injection of a pulse of 100  $\mu\text{Ci/kg}$  of [ $^{14}\text{C}$ ]deoxyglucose (specific activity, 50-55 mCi/mmol; New England Nuclear Corp., Boston, Mass.) contained in 3 ml of normal saline. In most of the animals, timed arterial blood samples were drawn during the ensuing 45 min period for the measurement of the arterial

§ To whom correspondence should be addressed.

plasma [ $^{14}\text{C}$ ]deoxyglucose and glucose concentrations required for eventual quantitation of local cerebral glucose utilization. Forty-five minutes after the pulse, the animal was killed by the intravenous injection of a large dose of sodium thiopental followed by a saturated solution of KCl sufficient to stop the heart. The animal was then decapitated, the extracranial soft tissues and lower mandible were removed as rapidly as possible, and the head was frozen in Freon XII chilled to  $-60^\circ$  with liquid nitrogen. With careful attention to keeping the tissues as cold as possible by repeated chilling in dry ice, the frozen head was cut into several pieces with a band saw, the brain portions were dissected free of bone, and the brain pieces were coated with embedding medium (Lipshaw Manufacturing Co., Detroit, Mich.), and fixed to object-holders appropriate to the microtome to be used. Brain pieces so prepared were stored in a freezer at  $-70^\circ$  until sectioned.

Brain sections, 20  $\mu\text{m}$  in thickness, were prepared in an American Optical Co. (Buffalo, N.Y.) cryostat maintained at  $-21^\circ$  to  $-22^\circ$ . The brain sections were picked up on glass cover slips, dried on a hot plate at  $60^\circ$ – $70^\circ$  for at least 5 min, and placed sequentially in an x-ray cassette. Autoradiographs were prepared from these sections directly in the x-ray cassette with Kodak single-coated blue-sensitive, Medical X-ray Film, Type SB-54 (Eastman Kodak Co., Rochester, N.Y.). The exposure time was generally about 5–6 days, and the exposed films were developed according to the instructions supplied with the film.

Three groups of animals with different conditions of visual input were studied: (i) intact binocular vision; (ii) bilateral visual occlusion; (iii) monocular visual occlusion. Visual occlusions were achieved either by enucleation or by insertion of opaque plastic discs in the appropriate eyes at the time of the surgical procedure for the insertion of the catheters. Animals with intact vision in one or both eyes were either exposed to the ambient light of the laboratory or surrounded by a black-white complex geometric pattern that was illuminated and rotated during the experimental procedure. The results were qualitatively similar with either method of visual occlusion and with or without the rotating geometric pattern.

## RESULTS

The autoradiographs obtained with the procedure used in these studies represent the distribution of [ $^{14}\text{C}$ ]deoxyglucose-6-phosphate in the tissues, and the concentration of this compound in a tissue reflects closely that tissue's rate of glucose utilization or energy metabolism (6, 7). The autoradiographs are, therefore, essentially pictorial representations of the relative rates of glucose consumption in the various anatomical components of the brain; the darker the region, the greater the rate of metabolism. Experimental modification of the visual input produced consistent changes in the pattern of distribution of the rates of energy metabolism which coincided closely with the changes in functional activity expected from known physiological and anatomical properties of the binocular visual system.

### Normal binocular vision

In animals with intact binocular vision no bilateral asymmetry was seen in the autoradiographs of the structures of the visual system (Figs. 1A and 2A). The lateral geniculate bodies and oculomotor nuclei appeared to be of fairly uniform density and essentially the same on both sides (Fig. 1A). Although not illustrated in this report, the optic nerves and tracts were clearly discernible in other autoradiographic sections; they exhibited the low densities characteristic of white matter and appeared



5.0mm

FIG. 1. Autoradiography of coronal brain sections at the level of the lateral geniculate bodies. Large arrows point to the lateral geniculate bodies; small arrows point to oculomotor nuclear complex. (A) Animal with intact binocular vision. Note the bilateral symmetry and relative homogeneity of the lateral geniculate bodies and oculomotor nuclei. (B) Animal with bilateral visual occlusion. Note the reduced relative densities, the relative homogeneity, and the bilateral symmetry of the lateral geniculate bodies and oculomotor nuclei. (C) Animal with right eye occluded. The left side of the brain is on the left side of the photograph. Note the laminae and the inverse order of the dark and light bands in the two lateral geniculate bodies. Note also the lesser density of the oculomotor nuclear complex on the side contralateral to the occluded eye.

to be bilaterally symmetrical. The visual cortex was essentially the same on both sides (Fig. 2A), but throughout all of Area 17 there was heterogeneous density distributed in a characteristic laminar pattern that distinguished it from the adjacent Area 18 and other regions of the cerebral cortex (Figs. 2A and 3). At least four different levels of density could be readily discerned which could be correlated with the known cytoarchitectural layers of the striate cortex apparent in myelin- and thionin-stained sections (Fig. 4). A wide band of relatively low but uniform density in the autoradiograph encompassed Layers I, II, and III which could not be distinguished further on the basis of [ $^{14}\text{C}$ ]deoxyglucose uptake (Fig. 4). Layers IVa, IVb, and IVc were clearly associated with high rates of glucose utilization as indicated by the density of the autoradiographic regions corresponding to them; Layers IVb and IVc were the most active, and exhibited the densest patterns of all layers seen in the autoradiograph (Fig. 4). When the autoradiograph is compared with the section stained for myelin, it appears that the line of Gennari lies within the layer with greatest metabolic activity (Fig. 4). In Layer V, there appears to be a fairly abrupt decline in density, but the activity in Layer VI is intermediate between those of Layers IV and V (Fig. 4). These observations indicate

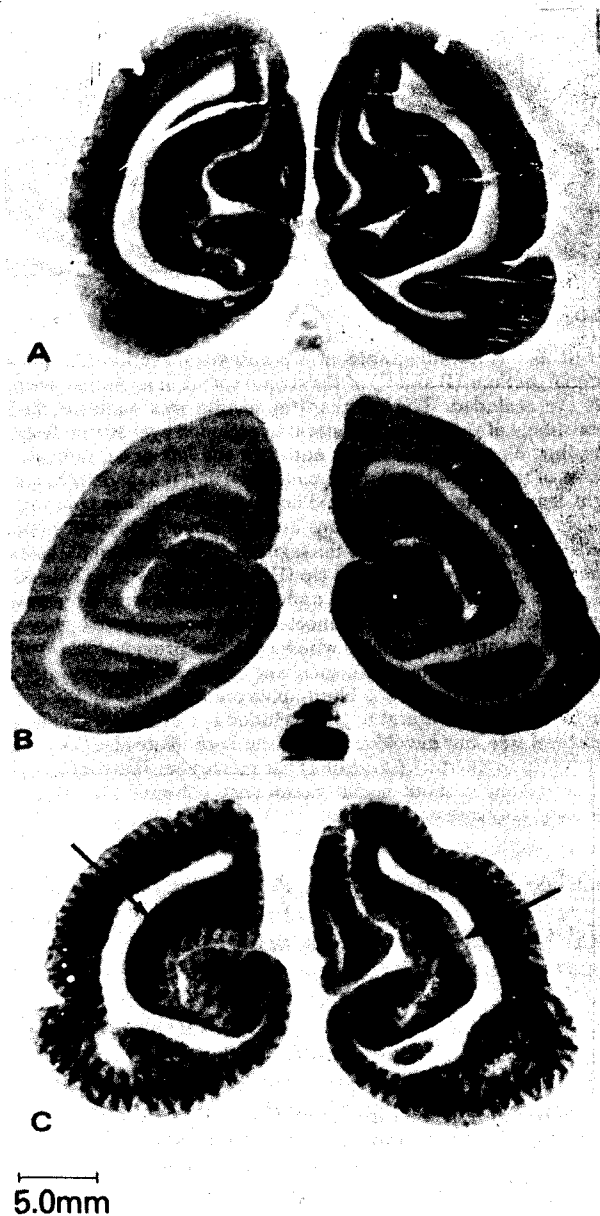


FIG. 2. Autoradiographs of coronal brain sections at the level of the striate cortex. (A) Animal with normal binocular vision. Note the laminar distribution of the density; the dark band corresponds to Layer IV. (B) Animal with bilateral visual deprivation. Note the almost uniform and reduced relative density, especially the virtual disappearance of the dark band corresponding to Layer IV. (C) Animal with right eye occluded. The half-brain on the left side of the photograph represents the left hemisphere contralateral to the occluded eye. Note the alternate dark and light striations, each approximately 0.3–0.4 mm in width that represent the ocular dominance columns. These columns are most apparent in the dark band corresponding to Layer IV, but extend through the entire thickness of the cortex. The arrows point to regions of bilateral asymmetry where the ocular dominance columns are absent. These are presumably areas with normally only monocular input. The one on the left, contralateral to occluded eye, has a continuous dark lamina corresponding to Layer IV which is completely absent on the side ipsilateral to the occluded eye. These regions are believed to be the loci of the cortical representations of the blind spots (see *text*).

that in animals with binocular visual input the rates of glucose consumption in the visual pathways are essentially equal on both sides of the brain and relatively uniform throughout the optic nerves, optic tracts, oculomotor nuclei, and lateral geniculate bodies but markedly different in the various layers of

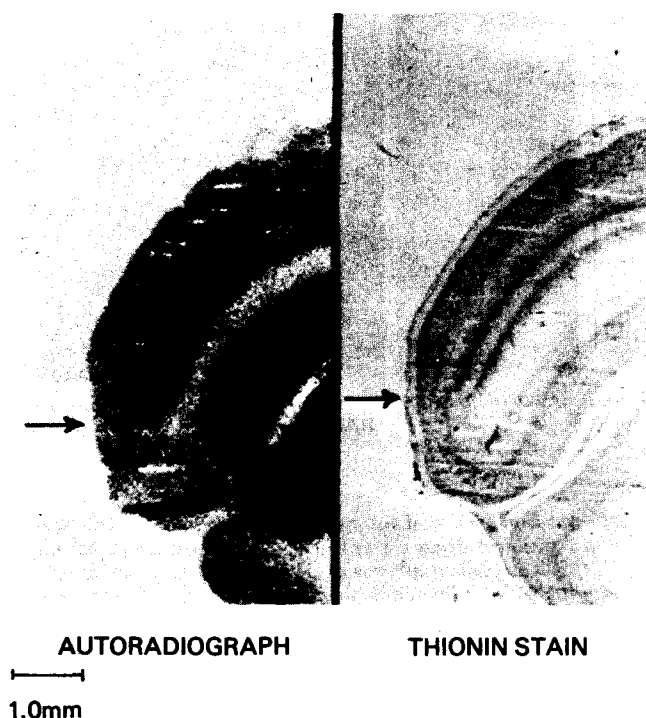


FIG. 3. Comparison of autoradiograph and thionin stain of a section of visual cortex at junction of Areas 17 and 18. The autoradiograph was made first from the frozen but undried brain section; the exposure of the film was carried out at  $-30^{\circ}$ . The section was then fixed and stained with thionin. The arrows point to the abrupt alteration of the cortical layers in the stained section and their autoradiographic representations in the autoradiographs at the junction of Areas 17 and 18.

the striate cortex. The most intense metabolic activity appears to be in sub-layers of Layer IV (Figs. 2A and 4) which coincide with the sites of termination of the geniculocortical projections on spine-bearing stellate cells (2, 8). Within each layer or sub-layer, however, the metabolic activity appears to be relatively uniform throughout the extent of the cortex representing the various portions of the visual fields.

#### Bilateral visual deprivation

Autoradiographs from the animals with both eyes occluded exhibited generally decreased labeling of all components of the visual system, but the bilateral symmetry was generally retained (Figs. 1B and 2B), and the density within each lateral geniculate body was for the most part fairly uniform (Fig. 1B). In the striate cortex, however, the marked differences in the densities of the various layers seen in the animals with intact bilateral vision (Fig. 2A) were virtually absent so that, except for a faint delineation of a band within Layer IV, the concentration of the label was essentially homogeneous throughout the striate cortex (Fig. 2B).

#### Unilateral visual deprivation

Autoradiographs from monkeys with only monocular input exhibited markedly different patterns from those described above. The optic nerve ipsilateral to the occluded eye showed less labeling than the contralateral nerve; the optic tracts exhibited bilateral symmetry, but both tracts were nonuniform with regions of higher density in the dorsolateral portions (autoradiographs not shown). Both lateral geniculate bodies exhibited exactly inverse patterns of alternating dark and light bands corresponding to the known laminae representing the

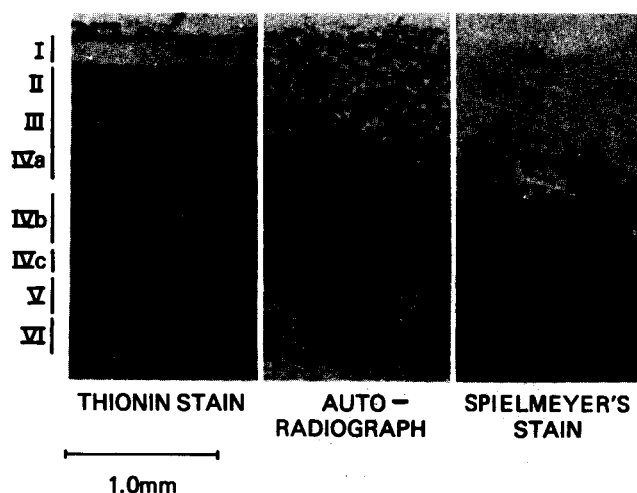


FIG. 4. Comparison of autoradiograph, thionin stain, and myelin stain of a section of striate cortex from a monkey with intact binocular vision. The autoradiograph was made from the same section subsequently stained with thionin by the procedure described in the legend to Fig. 3. An immediately adjacent section was stained for myelin with Spielmeyer's stain. The thionin stain distinguishes the cell-sparse Layers I, IVb, and V and the three cell-dense regions, Layers II, III and IVa (considered as one), Layer IVc, and Layer VI, according to Brodman's system. The dense zone in the autoradiograph traverses all of Layer IV and encompasses the stria of Gennari which is demarcated by the myelin stain. In some animals a thin dark band separate from Layer IV, possibly Layer IVa, could be discerned in the autoradiograph.

regions receiving the different inputs from the retinæ of the intact and occluded eyes (Fig. 1C). Bilateral asymmetry was also seen in the oculomotor nuclear complex; a lower density was apparent in the nuclei contralateral to the occluded eye (Fig. 1C). In the striate cortex the pattern of distribution of the [ $^{14}\text{C}$ ]deoxyglucose-6-phosphate appeared to be a composite of the patterns seen in the animals with intact and bilaterally occluded visual input. The pattern found in the former regularly alternates with that of the latter in columns oriented perpendicularly to the cortical surface (Figs. 2C and 5). The dimensions, arrangement, and distribution of these columns are identical to those of the ocular dominance columns described by Hubel and Wiesel (1-3). In a tangential section at the occipital pole, the columns appeared in cross section as dots arranged in parallel rows which seem to merge in Layer IV, where the labeling is most dense, giving the picture of a long palisade (Fig. 5B). The apparent increase in width of the columns in a few selected regions may reflect this merging as the plane of sectioning becomes parallel with the palisade (Fig. 5). The autoradiographs also confirm the conclusion reached from single cell recording techniques that the ocular dominance columns, although most prominent in Layer IV, also involve the entire cortical thickness (1); anatomic and [ $^{14}\text{C}$ ]proline and/or [ $^{14}\text{C}$ ]fucose autoradiographic techniques have demonstrated their distribution almost entirely in Layer IV (2-4).

There are two regions of the striate cortex where the ocular dominance columns are absent. These are regions known to have only monocular input even in animals with normal bilateral vision. One region is the rostral portion of the mushroom-like area of the calcarine cortex (Fig. 5A). This region receives input only from the most nasal crescent portion of the contralateral retina. Monocular occlusion removes all input and lowers [ $^{14}\text{C}$ ]deoxyglucose uptake in this region only on the contralateral side, but leaves the corresponding ipsilateral region

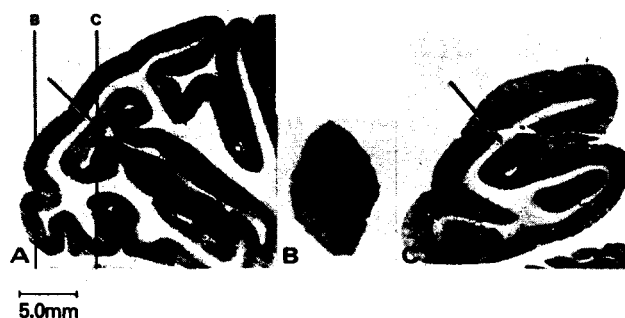


FIG. 5. Autoradiographs of a parasagittal section (A) and two coronal sections (B and C) of the striate cortex of an animal with the left eye occluded. The parasagittal section was made in the left hemisphere of the brain (ipsilateral to occluded eye) 10 mm from the mid-line. The lines marked B and C in the left panel indicate the planes of the coronal sections in panels (B) and (C) made through the right hemisphere of the brain. The ocular dominance columns are clearly visible in all the sections and are of generally the same dimensions and arrangement in the sagittal (A) and coronal (C) sections. The section near the occipital tip (B) transects the long axes of the columns, and they, therefore, appear as dots arranged in rows or stripes; some appear to be connected by a line as though they were slab-like in three dimensions which confirms previous observations obtained with electrophysiological and anatomical techniques (1, 2, 12). The cortical loci of the blind-spots are indicated by the arrows, low in density ipsilateral to the occluded eye and dark on the contralateral side, but devoid of columns in both. Note also the absence of columns in the rostral portion of the mushroom-like configuration. These regions without ocular dominance columns are areas with normally only monocular input.

unaffected (7). The other normally monocular regions are the loci of cortical representation of the blind spots of the visual fields. The area of the optic disc in the nasal half of each retina cannot transmit to this region of the contralateral striate cortex which, therefore, receives its sole input from an area in the temporal half of the ipsilateral retina. Occlusion of one eye deprives this region of the ipsilateral striate cortex of all input while the corresponding region of the contralateral striate cortex retains uninterrupted input from the intact eye. The metabolic reflection of this ipsilateral monocular input is seen in the autoradiographs in Fig. 2C and Fig. 5. The regions that we believe to be the loci of the representations of the blind-spots are located in the tops of the mushroom-like configurations of the folded cortex in the calcarine fissures. They are about 3 mm deep to the surface and involve a strip of cortex about 4 mm in length. They are devoid of ocular dominance columns. On the side contralateral to the occluded eye, this region gives the autoradiographic pattern of striate cortex with normal bilateral visual input; on the ipsilateral side, this region looks like striate cortex from an animal with totally deprived vision (Fig. 2C). We presume that these areas, which are so prominent in the autoradiographs, are the loci of the representations of the blind-spots because of their appropriate responses to the experimental conditions and their locations consistent with present knowledge of the cortical representation of the visual fields in the monkey (9).

## DISCUSSION

The results of these experiments not only confirm the structural and functional organization of the binocular visual system of the monkey established by painstaking electrophysiological and anatomic studies (1-3) but also provide a direct pictorial visualization of the distribution, nature, and extent of the regions of monocular representation throughout the brain. They also

demonstrate the effectiveness and potential usefulness of metabolic mapping by means of the [ $^{14}\text{C}$ ]deoxyglucose technique in the localization and delineation of brain loci with experimentally altered functional activity.

The binocular visual system has previously been visualized autoradiographically (3, 4), but by a method based on an entirely different principle from that underlying the [ $^{14}\text{C}$ ]deoxyglucose technique. The method used was the one based on the axoplasmic and trans-synaptic transport of [ $^3\text{H}$ ]proline and/or [ $^3\text{H}$ ]fucose-labeled protein and glycoprotein (10, 11). This method is dependent on anatomical continuity or contiguity and maps continuously only the anatomical pathway labeled from the site of injection of the tracer to its termination. Although trans-synaptic transport does occur, there is marked attenuation of the transfer of label at the synapse (10), and terminal segments of multi-synaptic pathways may, therefore, not be visualized. In contrast, the [ $^{14}\text{C}$ ]deoxyglucose technique maps all areas of the brain simultaneously on the basis of their local rates of glucose consumption and levels of functional activity. The method can detect regions of altered functional activity but provides no information about the anatomical pathways involved. Attenuation does not occur with this technique, and that is probably the reason why the [ $^{14}\text{C}$ ]deoxyglucose technique, in contrast to the axonal transport method, could confirm the findings of electrophysiological studies (1) that the ocular dominance columns in the striate cortex are not confined only to Layer IV but extend throughout the thickness of the cortex (Fig. 2C).

Like most autoradiographic methods both the axonal transport and the [ $^{14}\text{C}$ ]deoxyglucose techniques are subject to the problem of diffusion or migration of the labeled tracer from its original position *in situ*. Because its trapped labeled compound, [ $^{14}\text{C}$ ]deoxyglucose-6-phosphate, is water-soluble, the [ $^{14}\text{C}$ ]deoxyglucose method is particularly vulnerable to this problem. We have recently noted that diffusion of the label can occur in brain maintained at  $-15^\circ$  to  $-18^\circ$ . In a previous report (7) which contained an autoradiograph illustrating the cortical locus of the blind spot, this locus appeared as an ovoid structure extending through the entire thickness of the cortex, and the ocular dominance columns were poorly defined. There was clearly distortion due to diffusion. By meticulous attention to the storage of the frozen brain at  $-70^\circ$  and to its sectioning as rapidly as possible at  $-21^\circ$  to  $-22^\circ$ , we have been able to re-

duce the diffusion artifact and obtain autoradiographs with the resolution seen in this report. It is likely that even better resolution can be achieved by further refinements of the autoradiographic procedures.

Dr. M. H. Des Rosiers is a Fellow of Le Conseil des Recherches Médicales du Canada.

1. Hubel, D. H. & Wiesel, T. N. (1968) "Receptive fields and functional architecture of monkey striate cortex," *J. Physiol. (London)* **195**, 215-243.
2. Hubel, D. H. & Wiesel, T. N. (1972) "Laminar and columnar distribution of geniculate-cortical fibers in the Macaque monkey," *J. Comp. Neurol.* **146**, 421-450.
3. Wiesel, T. N., Hubel, D. H. & Lam, D. M. K. (1974) "Autoradiographic demonstration of ocular dominance columns in the monkey striate cortex by means of transneuronal transport," *Brain Res.* **79**, 273-279.
4. Rakic, P. (1976) "Prenatal genesis of connections subserving ocular dominance in the rhesus monkey," *Nature* **261**, 467-471.
5. Sokoloff, L., Reivich, M., Patlak, C. S., Pettigrew, K. D., Des Rosiers, M. & Kennedy, C. (1974) "The [ $^{14}\text{C}$ ]deoxyglucose method for the quantitative determination of local cerebral glucose consumption," *Trans. Am. Soc. Neurochem.* **5**, 85.
6. Sokoloff, L. (1975) "The [ $^{14}\text{C}$ ]deoxyglucose method for the quantitative determination of local cerebral glucose utilization," in *Blood Flow and Metabolism in the Brain*, eds. Harper, A. M., Jennett, W. B., Miller, J. D. & Rowan, J. O. (Churchill Livingstone, Edinburgh, Scotland), pp. 15.1-15.8.
7. Kennedy, C., Des Rosiers, M., Jehle, J. W., Reivich, M., Sharp, F. & Sokoloff, L. (1975) "Mapping of functional neural pathways by autoradiographic survey of local metabolic rate with [ $^{14}\text{C}$ ]deoxyglucose," *Science* **187**, 850-853.
8. Garey, L. J. & Powell, T. P. S. (1971) "An experimental study of the termination of the lateral geniculate-cortical pathway in the cat and monkey," *Proc. R. Soc. London* **179**, 41-63.
9. Daniel, P. M. & Whitteridge, D. (1961) "The representation of the visual field on the cerebral cortex in monkeys," *J. Physiol. (London)* **159**, 203-221.
10. Grafstein, B. (1971) "Transneuronal transfer of radioactivity in the central nervous system," *Science* **172**, 177-179.
11. Grafstein, B. (1973) "Transport of radioactivity from eye to visual cortex in the mouse," *Exp. Neurol.* **39**, 44-57.
12. LeVay, S., Hubel, D. H. & Wiesel, T. N. (1975) "The pattern of ocular dominance columns in Macaque visual cortex revealed by a reduced silver stain," *J. Comp. Neurol.* **159**, 559-576.